J Electroceram (2006) 17:9–14
DOI 10.1007/s10832-006-9928-7

Synthesis and UV-shielding properties of silica-coated calcia-doped ceria nanoparticles via soft solution processes

Ahmed Mohamed El-Toni · Shu Yin · Yuichiro Hayasaka · Tsugio Sato

Abstract White nanoparticles of calcia-doped ceria were prepared from the precipitate by reacting $CeCl_3$-$CaCl_2$ mixed solution with NaOH solution at pH 12 and the oxidation with hydrogen peroxide solution at 40°C, followed by the calcination at 700°C for 1 h. The sample before calcination contained significant amount of OH^- in the lattice and was yellow, but the powders calcined above 700°C were white, indicating that cation defect formed by replacing O^{2-} with OH^- played as the color center. It is confirmed that calcia-doped ceria showed much lower photocatalytic activity as well as lower generation of singlet oxygen under UV light irradiation than those with titania and zinc oxide. Calcia-doped ceria particles were coated with amorphous silica by means of sol-gel reaction technique using hydrolysis of tetraethylorthosilicate (TEOS) or acid hydrolysis of sodium silicate. The silica coating by sol-gel reaction with TEOS was much more efficient for the reduction of catalytic activity of ceria for the oxidation of organic materials without loss of UV-shielding ability than that by acid hydrolysis of sodium silicate.

Keywords Ceria · Calcia doping · Silica coating · UV-shielding · Oxidation catalytic activity

A. M. El-Toni · S. Yin · T. Sato (✉)
Institute of Multidisciplinary Research for Advanced Materials, Tohoku University, Sendai 980-8577, Japan
e-mail: tsusato@tager.tohoku.ac.jp

Y. Hayasaka
High Voltage Electron Microscope Laboratory, Tohoku University, Sendai, Japan

Introduction

The damaging effects of UV rays have been attracted attention and therefore various UV-shielding materials have been developed. Sun-care products incorporate many organic UV absorbents and inorganic UV filters, however, organic UV absorbents may pose a safety risk when used at high concentration. Fine particles of titania and zinc oxide are effective inorganic sunscreens widely used in personal-care products, but their high refractive indices can make the skin look unnaturally white. In addition, their high photocatalytic activity facilitates the generation of reactive oxygen species, raising safety concerns [1, 2]. Since the band gap energy of ceria is 3.1 eV being possible to filter out UV ray less than 400 nm wavelength and the value of the refractive index of ceria ($n = 2.05$) is lower than that of rutile ($n = 2.72$), anatase ($n = 2.5$) and zinc oxide ($n = 2.2$), it may have characteristics ideal for use in broad-spectrum inorganic sunscreen for personal-care products [3]. Many studies have reported the synthesis of nano-sized particles of ceria [4–7], however, because of its high catalytic activity for the oxidation of organic materials, ceria has seldom been commercially used as a sunscreen material. By doping with Ca^{2+} possessing lower valence and larger ionic size than those of Ce^{4+}, we succeeded in synthesizing novel nanoparticles of ceria with significantly reduced oxidation catalytic activity and possessing excellent UV absorption capability. Although ceriapowders are usually yellow, it is expected to make it white to use ceria as cosmetics and UV-shielding material for organic polymers. We tried to obtain white powder of ceria without loss of UV shielding ability by a soft solution chemical process followed by calcination at low temperature. In addition, the effect of silica coating method on the oxidation catalytic activity of ceria was investigated.

Experimental procedures

Preparation of white calcia-doped ceria powder: Nanoparticles of 20 mol% calcia-doped ceria ($Ce_{0.8}Ca_{0.2}O_{1.8}$) were prepared via soft solution chemical routes at 40°C as follows. At first 0.8 M $CeCl_3$ and 0.2 M $CaCl_2$ mixed aqueous solution and 3 M NaOH aqueous solution were simultaneously dropped into distilled water at 40°C with stirring to precipitate 20 mol% Ca^{2+}-doped $Ce(OH)_3$ at pH 12. Then, H_2O_2 aqueous solution was added to oxidize it to form $Ce_{0.8}Ca_{0.2}O_{1.8}$. Finally, the precipitates were washed with water and methanol and calcined at 700°C for 1 h.

Coating with amorphous silica: Calcia-doped ceria were coated with silica by two different methods, i.e., the sol-gel reaction of TEOS and acid hydrolysis of Na_2SiO_3. Silica coating by a sol-gel reaction of TEOS was conducted according to the previous papers [8–10] as follows. After dispersing calcia-doped ceria powder in TEOS/ethanol mixed solution, predetermined amount of water and 29 wt% ammonia aqueous solution were stepwise added. The molar ratio of TEOS:ethanol:water:ammonia were 1:100:400:10. The reaction time and temperature were 0.75 h and 40°C, respectively. On the other hand, silica coating by an acid hydrolysis of sodium silicate was conducted as follows. After dispersing calcia-doped ceria powder in sodium silicate aqueous solution, sulfuric acid (pH = 1) was dropped till pH reaches 5. The slurry was stirred for 0.75 h. The precipitates obtained by both methods were filtered, washed and dried at 80°C overnight.

Analysis: The morphology of the powder was examined using a transmission electron microscope (JEOL, JEM-3010). The crystalline phase identification was performed by the powder X-ray diffraction (Rigaku, XD-01) using graphite monochromatized CuKα radiation. The BET specific surface area was determined by nitrogen adsorption analysis (NOVA, 1000TS). The amount of water was determined by gravimetric method by calcination. The powder density was determined using a pycnometer and i-propanol.

Evaluation of oxidation catalytic activity: The catalytic activity for the oxidation of organic material was determined using the conductometric determination method (Rancimat System, Metrohm E679) [11–13]. One gram of the sample powder was mixed with 10 g of castor oil and heated to 120°C while bubbling air at 0.5 dm^3 min^{-1}, where the air was introduced into distilled water attached to an electric conductivity measurement cell. The catalytic activity was evaluated by measuring the increase in the conductivity of distilled water resulting from trapping of volatile molecules formed by the oxidation of castor oil on heating.

Evaluation of photocatalytic activity: The photocatalytic activity was evaluated by measuring the degree of decomposition of *p*-methoxycinnamic acid 2-ethylhexyl ester and 4-t-buthyl-4'-methoxybenzoilmethane which are commercially used as UV absorber by irradiating sunlight to the solution consisting of 8 g p-methoxycinnamic acid 2-ethylhexyl ester, 1 g 4-t-buthyl-4'-methoxybenzoilmethane, 30.5 g decamethylcyclopentasiloxane, 10 g trioctanoic acid glyceril and 0.5 g sample powder at room temperature using a Gas Chromatograph Mass Spectrometer (Shimadzu GCMS-QP2010).

Evaluation of the production of singlet oxygen by photoirradiation: The low-level intensity of chemiluminescence of singlet oxygen, $^1O_2$, was directly measured with a chemiluminescence analyzer (Tohoku Electric Ind., CLA-FC2). Approximately 3 g of the sample powder was placed into a stainless steel cell (50 mm in diameter and 10 mm in depth) covered with a quartz cell. A 6 W UVA/B fluorescent tube (UVP, UVGL-58) was used as the light source. The test sample was irradiated in air with UV ray of 254 nm for 5 sec at room temperature. Chemiluminescence intensity was measured 5 s later for 100 s, where a red filter transmitting only light of wavelength greater than 600 nm was placed between the cuvette and the photomultiplier to cut off the emission attributed to carbonyl compounds.

Evaluation of UV shielding property: The UV-shielding property of the particle was evaluated by measuring the transmittance of the film consisting of uniformly dispersed sample powder with a UV-Vis spectrophotometer (Shimadzu, UV-2500PC), where 2 g of sample powder, 4 g of industrial grade nitrocellulose, 10 g of ethyl acetate and 9 g of butyl acetate were mixed uniformly using paint shaker (Asada) and 100 g of zirconia ball (2.7 mm in diameter) for 24 h. The dispersion mixture was applied onto a quartz glass plate with an applicator. Thickness of the film was 3 μm after drying at room temperature for 24 h.

Results and discussion

Although the ceria powder before calcination was yellow, it turned to white by calcination above 700°C. The TG-DTA curves of as-prepared ceria are shown in Fig. 1. The powder

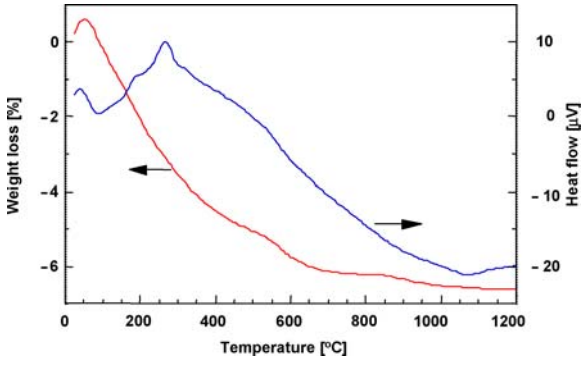

Fig. 1 TG-DTA curves of CeO_2 before calcination

Table 1 Weight loss by heating up to 1200°C, x in $Ce_{1-x/4}O_{2-x}(OH)_x$, lattice constant, a, and calculated and determined density of the calcined powder

Calcined temp. [°C]	Weight loss [%]	x	a [nm]	Density [g · cm^{-3}] Found	Calcd.
200	5.89	0.920	0.5430	5.90	5.60
300	4.28	0.704	0.5440	6.21	5.75
400	3.42	0.579	0.5418	6.38	6.40
500	2.89	0.547	0.5415	6.43	6.45
600	2.41	0.422	0.5414	6.61	6.60
700	1.22	0.223	0.5413	6.89	6.88
800	0.38	0.071	0.5414	7.13	7.13

showed large weight loss (ca. 6%) up to 700°C and then the weight was almost constant. Since surface-adsorbed water is usually released until 200°C, it is suspected that as-prepared ceria contained OH^- in the lattice. Similar phenomena have been observed for the hydrothermally prepared $Zr_{0.5}Ce_{0.5}O_2$ solido solution, i.e., the samples had larger lattice parameters since the samples possess OH^- ions in the lattice [14, 15]. When O^{2-} is substituted with OH^-, the cation defect may be formed for the charge compensation as shown by $Ce_{1-x/4}O_{2-x}(OH)_x$.

In order to confirm the crystal structure of ceria, as-prepared ceria powder was calcined at various temperatures for 1 h. The lattice constant decreased with increasing calcination temperature to approach the reported value of CeO_2 (0.5411 nm: JCPDS 34-394). By assuming that the surface-adsorbed water and OH^- in the lattice are completely released until 200 and 1200°C, respectively, the value of x and theoretical density of calcined sample were calculated according to the chemical formula of $Ce_{1-x/4}O_{2-x}(OH)_x$ as shown in Table 1. The densities calculated agreed well with determined density by pycnometry and both values approached the value of CeO_2 (7.215 g · cm^{-3}: JCPDS 34-394) with increasing calcination temperature. These results indicate that the cation vacancy formed by incorporating OH^- plays as a color center to show yellow color.

Figure 2 shows the photocatalytic activity of calcia–doped ceria for the decomposition of organic UV absorbents together with that of cosmetic grade titania coated with 5.5 wt% SiO_2 and 3 wt% $Al(OH)_3$, and zinc oxide where the surface areas of them were 101, 44.7 and 42.8 m^2 · g^{-1}, respectively. It is seen that both organic UV-absorbers were significantly decomposed in the presence of zinc oxide and titania, whereas the decomposition of them in the presence of calcia-doped ceria was negligibly small, indicating the photocatalytic activity for the decomposition of UV absorbent was in the order of zinc oxide > titania > calcia-doped ceria although calcia-doped ceria possessed the greatest specific surface area.

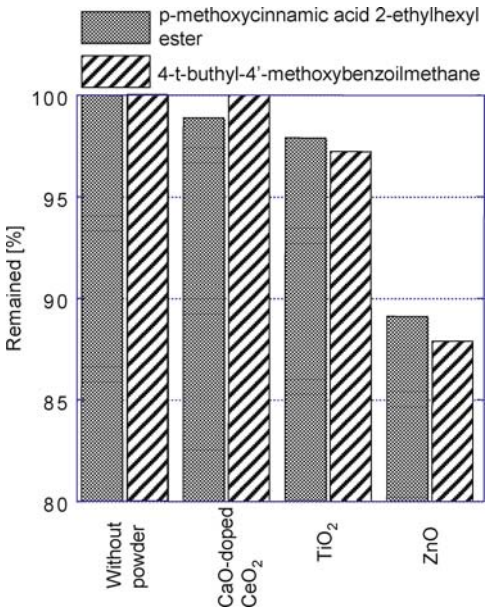

Fig. 2 *p*-Methoxycinnamic acid 2-ethylhexyl ester and 4-t-buthyl-4′-methoxybenzoilmethane remained after irradiation of sunlight for 1 day at room temperature

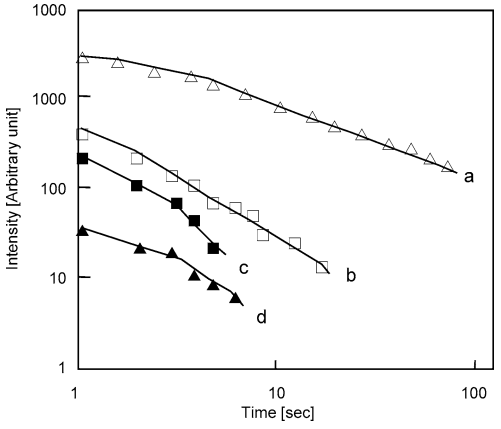

Fig. 3 Chemiluminescence caused by singlet oxygen by irradiating with UV rays. (a) ZnO, (b) TiO_2, (c) CeO_2 and (d) $Ce_{0.8}Ca_{0.2}O_{1.8}$

Singlet oxygen has so-called dimol emission (i) and monomol emission (ii) [16];

$$^1O_2 + {}^1O_2 \rightarrow 2\,^3O_2 + h\nu \quad (634 \text{ and } 703 \text{ nm}) \qquad \text{(i)}$$

$$^1O_2 \rightarrow {}^3O_2 + h\nu \quad (1270 \text{ nm}) \qquad \text{(ii)}$$

We monitored very weak chemiluminescence in the visible ray region (600–850 nm) using a red filter to cut off the emission attributed to carbonyl compounds [17]. The intensity of chemiluminescence emission of $^1O_2$ generated by the irradiation of UV rays is shown in Fig. 3. Although several studies have reported on the lifetime of $^1O_2$ in various kinds of solvents, there has been no report on the lifetime of $^1O_2$ produced by photo-irradiation of a semiconductor in

air. Quite long duration for the decay of chemiluminescence was observed. It was indicated that there were quite fewer amounts of $^1O_2$ generation on the surface of both undoped ceria and calcia-doped ceriathan that on zinc oxide and titania. In addition, initial emission intensities of calcia-doped ceria was less than 20% of that of undoped ceria. The low $^1O_2$ generation on calcia-doped ceria may be due to the existence of an oxygen defect formed by doping with calcia, since it is known that the oxygen defect plays an important role in enhancing the recombination reaction of photoinduced electron and hole. Even undoped ceria itself has a tendency to form an oxygen defect, by doping with calcia the amount of the oxygen defect must greatly increase.

Typical TEM micrographs showed that calcia-doped ceria calcined at 700°C consisted of nanoparticles with a size distribution between 10–15 nm (Fig. 4(a)). High resolution TEM micrograph for 10 wt.% silica-coated calcia-doped ceria for 3 h (Fig. 4(b)) clearly showed that the calcia-doped ceria crystals were coated with amorphous silica shell of 2–5 nm thickness although the particles were agglomerated.

Figure 5 shows XPS O1s core level spectra of non-coated and silica-coated calcia-doped ceria together with that of silica. It is clear that different kinds of oxygen are present. For non-coated calcia-doped ceria (Fig 5(a)), a large one at 528.8 eV was attributed to lattice oxygen ions in calcia-doped ceria, and a smaller one at 531 eV was attributed to adsorbed oxygen. For silica-coated calcia-doped ceria (Fig. 5(b)–(d)), peak at 533.1 eV was attributed to silica and the other one at 529.5 eV was attributed to calcia-doped ceria. Silica-coated calcia-doped ceria by sol-gel reaction using TEOS showed higher peak intensity of silica than that by acid hydrolysis of sodium silicate, indicating that silica content in the sample prepared using sodium silicate precursor was lower than that prepared with TEOS. It is notable that the 529.5 eV peak of O 1s in silica-coated calcia-doped ceria resulted from a chemical shift of 528.8 eV peak of O 1s in pure calcia-doped ceria. In the coated calcia-doped ceria powder, it is inferred that Si is combined onto the surface of calcia-doped ceria, forming a Ce–O–Si bond.

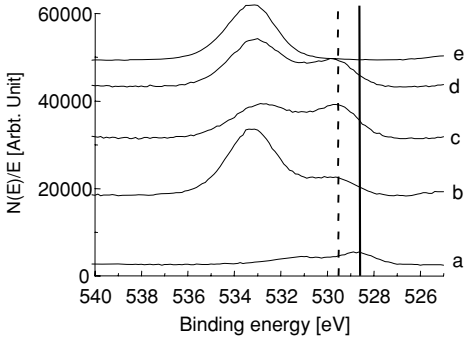

Fig. 5 O 1s XPS spectra of (a) non-coated calcia doped ceria, calcia doped ceria coated with (b) 20 wt% silica by seeded polymerization using TEOS (0.75 h), (c) 20 wt% silica by acid hydrolysis of sodium silicate (0.75 h) and (d) 10 wt% silica by seeded polymerization using TEOS (3 h), and (e) silica

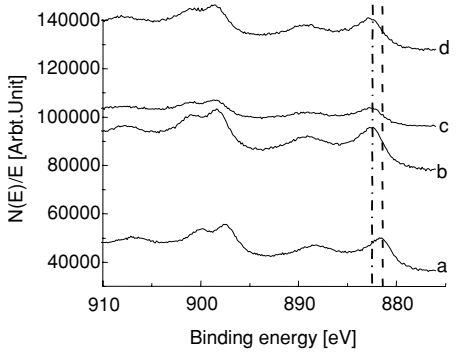

Fig. 6 Ce 3d XPS spectra of (a) non-coated calcia-doped ceria, calcia-doped ceria coated with (b) 20 wt% silica by seeded polymerization using TEOS (0.75 h), (c) 20 wt% silica by acid hydrolysis of sodium silicate (0.75 h), and (d) 10 wt% silica by seeded polymerization using TEOS (3 h)

Because the electronegativity of Si is greater than that of Ce, O 1s peak for calcia doped ceria has a chemical shift of +0.7 eV.

XPS $Ce3d_{5/2}$ core level spectra of non-coated and silica coated calcia doped ceria are shown in Fig. 6. With comparing the spectra of non-coated (Fig. 6(a)) and silica-coated calcia-doped ceria (Fig. 6(b)–(d)), the result revealed that binding

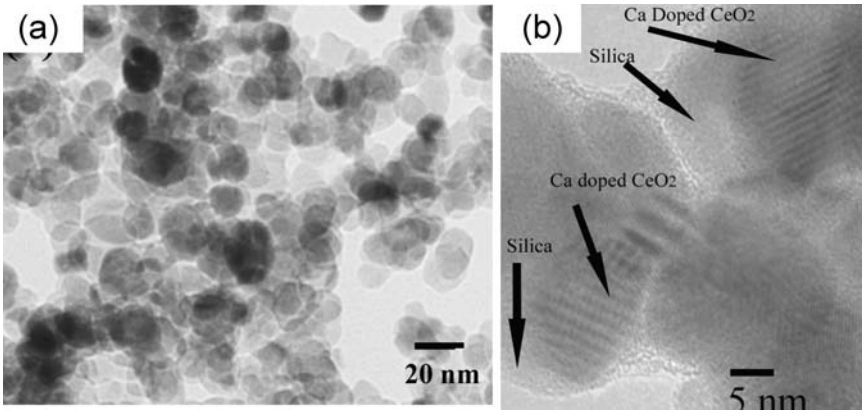

Fig. 4 (a) TEM micrographs of calcia-doped ceria calcined at 700°C before silica coating and (b) High resolution TEM micrograph of 10 wt.% silica-coated calcia-doped ceria for 3 h

energy of $Ce3d_{5/2}$ peak was shifted from 881.3 to 882.5 eV by silica-coating, i.e., the binding energy of $Ce3d_{5/2}$ peak of silica-coated calcia-doped ceria is 1.2 eV greater than that of $Ce3d_{5/2}$ peak of non-coated calcia-doped ceria. It is also an evidence for deducing that Ce–O–Si bond forms. The decrease of the electron density around Ce atom results from the greater electronegativity of Si via O acting on Ce. The shielding effect is weakened, and then the binding energy is increased.

As expected, the catalytic ability of calcia-doped ceria for air oxidation of castor oil at 120°C was decreased substantially by coating with silica shell using both seeded polymerization and acid hydrolysis techniques as shown in Fig. 7. It can be observed that coating by sol-gel reaction using TEOS precursor delayed the oxidation of castor oil more effectively than using acid hydrolysis of sodium silicate one. This can be attributed to that silica coating using TEOS helped to cover the surface of calcia-doped ceria uniformly while sodium silicate coating usually covered the surface in a patch-wise and non-uniform manner [18].

In order to evaluate the UV shielding ability of non-coated and silica-coated calcia-doped ceria, the UV-Vis transmittance spectra of the samples were determined and the results are shown in Fig. 8. Non-coated calcia-doped ceria showed excellent UV-shielding ability and transparency in the visible light region. Silica-coated samples using sodium silicate and TEOS possessed similar transparency in the visible light region but their UV-shielding decreased due to the decrease in ceria content. UV-shielding for calcia-doped ceria coated with 5 wt.% silica for 3 h shows identical properties to non-coated calcia-doped ceria. Calcia-doped ceria coated with 20 and 10 wt.% silica by sol-gel reaction technique for 0.75 h and 3 h, respectively, have comparable UV shielding properties. This can be attributed to the fact that increasing coating time can leads to increment of precipitation of silica from solution.

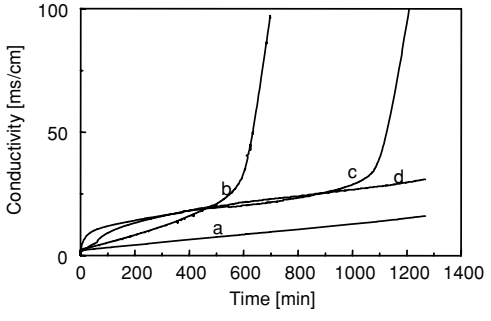

Fig. 7 Evaluation of oxidation catalytic ability at 120°C with the Rancimat systems. (a) Blank (without sample), (b) non-coated calcia-doped ceria, calcia-doped ceria coated with (c) 20% silica by acid hydrolysis of sodium silicate (0.75 h) and (d) 20% silica by seeded polymerization using TEOS (0.75 h)

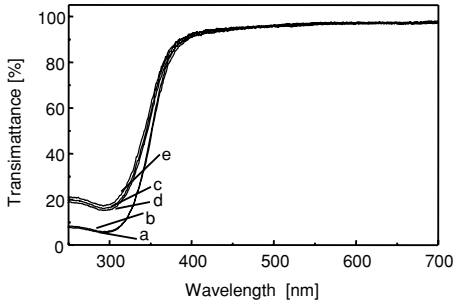

Fig. 8 UV-Vis transmittance spectra of thin films of (a) non-coated calcia-doped ceria , calcia-doped ceria coated with (b) 5 wt% silica (3 h), (c) 10 wt% silica (3 h), (d) 20 wt% silica (0.75 h) by seeded polymerization using TEOS and (e) 20 wt% silica by acid hydrolysis of sodium silicate (0.75 h)

Conclusion

Nanoparticles of ceria were prepared via soft solution chemical routes. The color of the powder can be change from yellow to white without excess grain growth by calcination at low temperature around 700°C. The photocatalytic activity of calcia-doped ceria was much lower than that of titania and zinc oxide. The generation of singlet oxygen on ceria with UV irradiation in air was also lower than that on titania and zinc oxide and was greatly decreased by doping with calcia. The catalytic ability of calcia-doped ceria for air oxidation of castor oil was decreased substantially by coating with silica shell using sol-gel reaction of TEOS and acid hydrolysis of sodium silicate. Coating of calcia-doped ceria with silica by seeded polymerization using TEOS precursor delayed the oxidation of castor oil more effectively than that using acid hydrolysis of sodium silicate. Silica coated samples by acid hydrolysis and sol-gel reaction techniques possessed transparency in the visible light region but their UV shielding ability decreased slightly due to the decrease in ceria content. Sol-gel reaction coating showed better UV-shielding ability than acid hydrolysis of sodium silicate.

Acknowledgment This research was partially supported by the Ministry of Education, Culture, Sports, Science and Technology, a Grant-in-Aid for the Scientific Research of Priority Areas (Panoscopic Assembling and High Ordered Functions for Rare Earth Materials) and the Cosmetology Research Foundation.

References

1. R. Cai, K. Hashimoto, K. Itoh, Y. Kubota, and A. Fujita, *Bull. Chem. Soc. Jpn.*, **64**, 1268 (1991).
2. Y. Yamamoto, W.C. Dunlap, N. Imai, R. Mashita, R. Konaka, M. Inoue, Y. Hasegawa, and T. Miyoshi, *Proceedings of 20th IFSCC Congress Canes*, **1**, 153 (1998).
3. S. Yabe and S. Momose, *J. Soc. Cosmet. Chem. Jpn.*, **32**, 372 (1998).
4. P. Chen and I. Chen, *J. Am. Ceram. Soc.*, **76**, 1577 (1993).

5. M. Hirano and E. Kato, *J. Am. Ceram. Soc.*, **79**, 777 (1996).
6. T. Masui, K. Fujikawa, K. Machida, T. Sakata, H. Mori, and G. Adachi, *Chem. Mater.*, **9**, 2197 (1997).
7. X. Yu, F. Li, X. Ye, X. Xin, and Z. Xue, *J. Am. Ceram. Soc.*, **83**, 964 (2000).
8. W. Stöber, A. Fink, and E. Bohn, *J. Colloid Interf. Sci.*, **26**, 62 (1968).
9. Y. Kobayashi, K. Misawa, M. Kobayashi, M. Takeda, M. Konno, M. Satake, Y. Kawazoe, N. Ohuchi, and A. Kasuya, *Coll. Surf. A: Physicochem. Eng. Aspects*, **242**, 47 (2004).
10. Y. Kobayashi, K. Misawa, M. Takeda, M. Kobayashi, M. Satake, Y. Kawazoe, N. Ohuchi, A. Kasuya, and M. Konno, *Coll. Surf. A: Physicochem. Eng. Aspects* **251**, 197 (2004).
11. J. Frank, J.V. Geil, and R. Freaso, *Food Technol.*, **36**, 71 (1982).
12. M.W. Laubli and P.A. Bruttel, *J. Amer. Oil Chem. Soc.*, **63**, 792 (1986).
13. C. Kato and K. Makabe, *J. Jpn. Oil Chem. Soc.*, **42**, 55 (1993).
14. A. Ahniyaz, T. Fujiwara, T. Fujino, and M. Yoshimura, *J. Nanosci. Nanotechnol.*, **4**, 233 (2004).
15. A. Ahniyaz, T. Watanabe, and M. Yoshimura, *J. Phys. Chem. B*, **109**, 6136 (2005).
16. J.R. Kanofsky, *Chemico-Biological Interactions*, **70**, 1 (1989).
17. T. Miyazawa, K. Fujimoto, M. Kinoshita, and R. Usuki, *J. Amer. Oil Chem. Soc.*, **71**, 343 (1994).
18. Q. Liu, Z. Xu, J.A. Finch, R. Egerton, *Chem. Mater.*, **10**, 3936 (1998).